JOURNAL OF MATERIALS SCIENCE 19 (1984) 3835–3843

On the ageing of an aluminium–lithium–zirconium alloy

P. LOUISE MAKIN, BRIAN RALPH*
Department of Metallurgy and Materials Science, University of Cambridge, UK

Electron microscopy has been used to follow the ageing of an aluminium alloy containing 3.08 wt % lithium and 0.19 wt % zirconium over the temperature range 433 to 553 K. A dispersion of Al_3Zr particles was present before these ageing treatments and is unmodified by them. Two dispersions of Al_3Li (δ') are produced by these ageing treatments, one is formed homogeneously in the matrix while the other nucleates and coarsens on the Al_3Zr/matrix interface. From the data it appears that there is little interaction between the lithium and zirconium in solution and that the precipitation processes occur chemically independently. The coarsening characteristics of both dispersions of δ' have been investigated as has the discontinuous precipitation of δ'.

1. Introduction

The aluminium–lithium system has been the subject of a large amount of technological interest in the last decade or so because it presents an opportunity to develop an alloy with good specific properties (e.g. [1, 2]). The addition of each wt % lithium (up to a maximum of 4 wt %) to an aluminium alloy decreases the density approximately 3% and increases the elastic modulus by approximately 6% (e.g. [3]). High yield strengths can be achieved by the nucleation and growth of a coherent metastable δ' precipitate that forms on low temperature ageing (e.g. [4]). At present, the ductility of the alloys is the source of some concern in the development programmes as the alloys suffer from intragranular fracture, thus work is being done using alloying additions and thermomechanical processing in an attempt to alter the precipitation characteristics and decrease the grain size of the alloys (e.g. [5]).

The influence of small amounts of zirconium on high strength aluminium alloys is well known, not only for its effects of retarding recrystallization and controlling grain growth, but also from the associated improvement in toughness, stress-corrosion resistance and quench sensitivity resulting from its addition. It is widely believed that these improvements are due to a high density of metastable cubic Al_3Zr precipitates (e.g. [6]).

The present study is part of an investigation into the effects of the addition of zirconium on the characteristics of the Al–Li binary system. Using a simple Al–Li–Zr ternary alloy, the direct effect of the addition of zirconium on binary alloy characteristics can be seen without the complications arising from the use of further alloying additions. The results obtained can then be applied to the development of zirconium-containing commercial aluminium–lithium alloys.

The precipitation characteristics of the Al–Li binary system have been investigated by several workers (e.g. [4, 7]) and they were recently reviewed at the first international conference devoted to the Al–Li systems [8]. The region of the phase diagram of interest is that with a lithium content of less than 4% Li, as this is the limit of total lithium solubility in aluminium. The phases present in this region are α, Al–Li solid solution, lattice parameter = 0.404 nm; δ, Al–Li equilibrium intermetallic, B32 cubic structure with a lattice parameter of 0.637 nm and δ', Al_3Li metastable phase, LI_2 cubic structure with a lattice parameter of 0.4038 nm.

In a 3% Li binary alloy, the latter phase forms

*Present address: Department of Metallurgy and Materials Science, University College, Cardiff, UK.

0022–2461/84 $03.00 + .12

homogeneously throughout the matrix with a cube/cube orientation relationship on quenching and is stable up to a temperature of 553 K. The coarsening of this matrix δ' has been shown to obey Lifschitz–Wagner kinetics in the temperature range 413 to 473 K with the change in average radius, r, being proportional to $(\text{time})^{1/3}$ [7]. The coarsening of δ' at defects such as dislocations or boundaries has also been observed, the latter effect being an example of a discontinuous reaction where lammellae of δ' are produced behind a migrating boundary [9].

The stable δ phase is thought to nucleate independently of the δ' on heterogeneities such as dislocations or boundaries, and it has been seen after relatively long ageing times with the associated generation of a large number of interfacial dislocations. Subsequent growth occurs by the dissolution of surrounding δ' particles leading to a δ' precipitate-free zone around δ particles [7].

Nes reported the precipitation characteristics of an Al–0.18% Zr alloy [6]. He found that the precipitating phase was the metastable cubic Al_3Zr which has an LI_2 structure and formed in a cube/cube orientation relation with the matrix. The lattice constant of the precipitate was calculated as 0.408 nm after the precipitate/matrix misfit had been measured as $0.8 \pm 0.1\%$. No precipitation was detected for annealing times of less than 24 h at 733 K and during annealing at this temperature, the precipitate was found to be stable to a maximum time range of 700 h. The nucleation mechanism was always found to be heterogeneous on dislocations and boundaries, and the morphology of the precipitates was mostly spherical although rod-shaped precipitates oriented in ⟨100⟩ matrix directions and plates on {100} matrix planes were also observed.

2. Experimental details

The alloy used in this work had the composition Al–3.08% Li–0.19% Zr and was prepared by the Alcan International Research Laboratories, Banbury, UK. After casting, the alloy was homogenized in a furnace at 833 K for 24 h, and then hot cross-rolled to a thickness of 19 mm. After a solution heat treatment at 883 K for 20 h, the ageing treatments described in Table I were performed. All heat treatments were terminated by a quench into water at 293 K, and were performed in air. The dimensions of the heat treated specimens were greater than 15 mm in order to avoid the effects resulting from lithium loss during the treatments, as transmission electron microscope foils were prepared from material cut from the centre of these bulk specimens.

TABLE I

Temperature (K)	Time (min)	(h)	(h)	(h)	(h)
433	30	4	20	48	–
443	30	4	20	48	–
453	30	4	20	48	–
473	30	4	20	48	–
513	30	4	20	48	–
553	30	4	20	48	96

The foils were polished in a solution of 30% nitric acid in methanol at a temperature of 243 K and a voltage of 9 V and then examined within 2 h in either Philips 300, 400ST or 400T microscopes. All precipitate size measurements were made on centred dark-field micrographs which had been taken using a superlattice reflection, and regression analysis was used to calculate the "best fit" lines on the coarsening plots made.

3. Results

The solution heat treated microstructure appeared to be recovered, consisting of approximately 5 μm subgrains. Spherical Al_3Zr precipitates ranging in size from 30 to 100 nm diameter were visible both within the grains and pinning subgrain boundaries. Fig. 1a shows a typical dispersion of Al_3Zr particles after this treatment. No δ' precipitate can be resolved but it is not possible to determine whether any had formed on quenching due to the coincidence of the δ' and Al_3Zr superlattice spots resulting from their similar lattice parameters and orientation relationships to the matrix. The subsequent ageing treatments used to precipitate δ' left the Al_3Zr dispersion unchanged.

3.1. Formation of δ'

After 30 min at each of the ageing temperatures specified, δ' was observed to be distributed homogeneously throughout the matrix. Precipitation was also observed on the Al_3Zr/matrix interface. At the lower ageing temperatures it appeared that this consisted of distinct precipitates of a size comparable to the matrix δ' as shown in Fig. 1b where the Al_3Zr particle A is surrounded by an incomplete shell of small δ' precipitates. The same

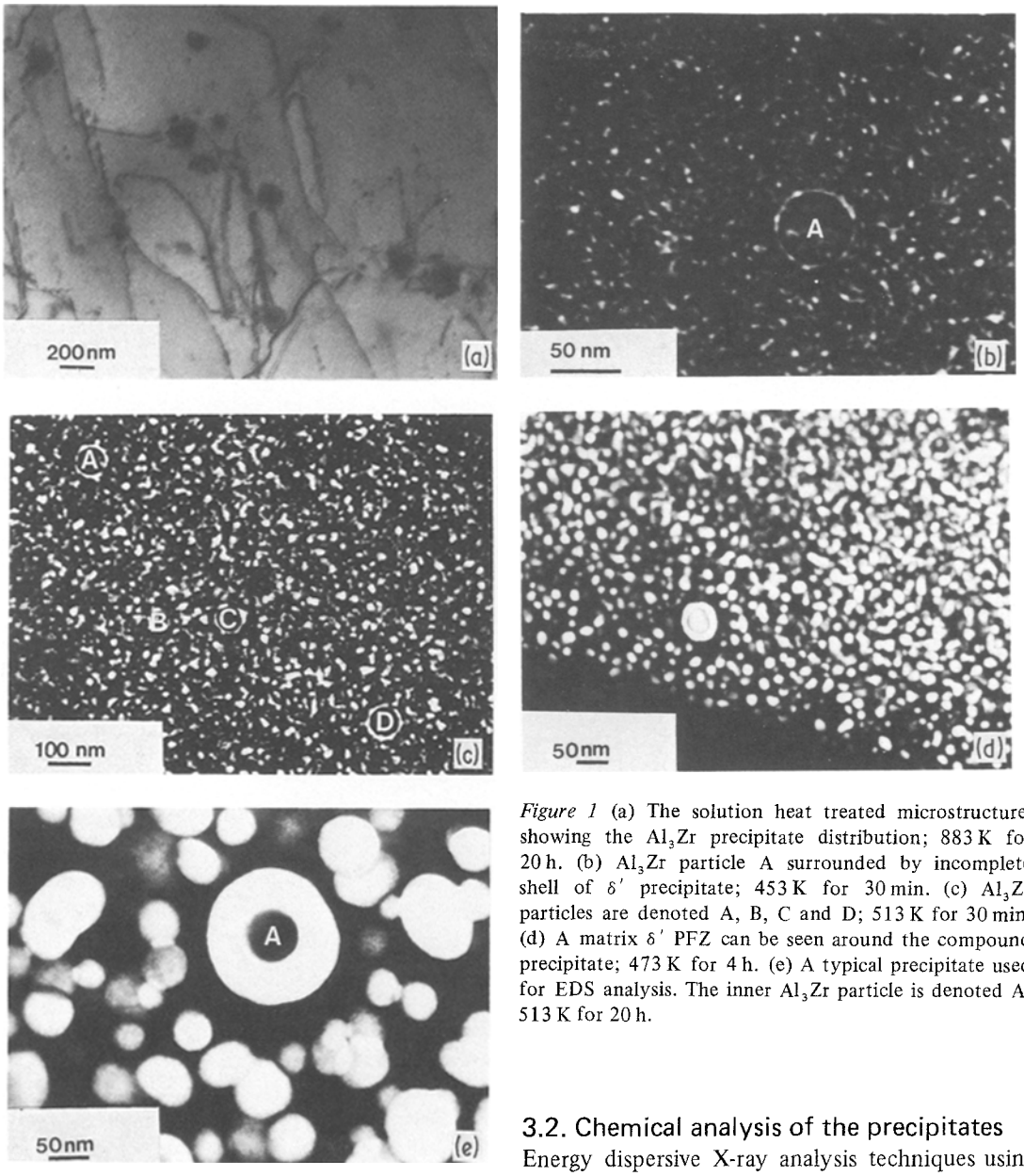

Figure 1 (a) The solution heat treated microstructure, showing the Al_3Zr precipitate distribution; 883 K for 20 h. (b) Al_3Zr particle A surrounded by incomplete shell of δ' precipitate; 453 K for 30 min. (c) Al_3Zr particles are denoted A, B, C and D; 513 K for 30 min. (d) A matrix δ' PFZ can be seen around the compound precipitate; 473 K for 4 h. (e) A typical precipitate used for EDS analysis. The inner Al_3Zr particle is denoted A; 513 K for 20 h.

time at a higher temperature (Fig. 1c) had caused a more continuous film of precipitate to be formed around the Al_3Zr precipitates (A, B, C and D), but again it appeared to consist of precipitates of a similar size to the surrounding matrix δ'. The precipitation of the δ' on the Al_3Zr/matrix interface appeared not to modify the surrounding matrix δ' distribution for samples aged for 30 min at all the ageing temperatures investigated.

3.2. Chemical analysis of the precipitates

Energy dispersive X-ray analysis techniques using an electron probe size of ~ 1 nm were used to analyse the compound precipitates for the presence of zirconium. A specimen that had been aged for 20 h at 513 K was used, and the precipitates analysed had an inner diameter of the order of 50 nm with the width of the surrounding precipitate shell being of a similar size (Fig. 1e). The traces obtained from these two regions of precipitate are shown in Fig. 2, from which it can be seen that there appears to be a significant amount of zirconium in the inner region of the precipitate, yet none in the outer shell. It was concluded that the outer shell probably con-

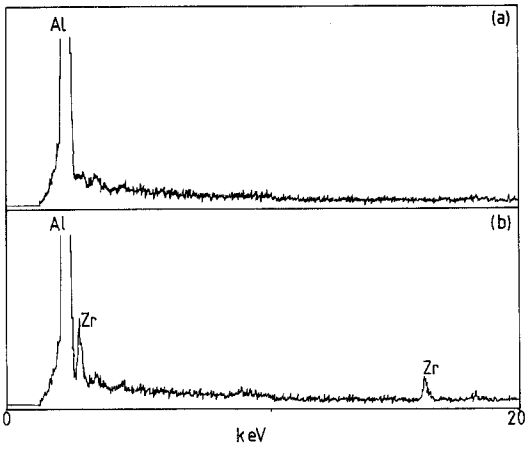

Figure 2 EDS traces obtained from (a) outer rim, (b) inner particle of a compound precipitate similar to that seen in Fig. 1e.

sisted of δ' precipitate similar to that formed in the matrix. Further work is in progress using an electron energy loss technique to measure the amounts of lithium present within the two regions of the precipitate and the matrix.

3.3. Coarsening of δ'

For all the ageing temperatures employed, the matrix δ' increased in size whilst decreasing in number density with increasing ageing time. The interfacial δ' precipitate eventually formed a complete shell around the Al_3Zr precipitate and on ageing this increased in width symmetrically around Al_3Zr particles within the subgrains. Fig. 1d shows a compound precipitate surrounded by a complete shell of δ' precipitate in an area near to the edge of the foil. A matrix δ' precipitate free zone (PFZ) can be seen around this compound precipitate and this was seen around many other coarsened compound precipitates in thin areas of the specimens. In the thicker regions, the high volume fraction of matrix precipitate lead to much overlap of the images and obscured any PFZ which may have been present. Fig. 1e shows a compound precipitate at a more advanced stage of coarsening, from which it can be seen that the width of the shell has now exceeded the radius of the inner Al_3Zr precipitate A, and the compound precipitate is still of a larger overall radius than any of the matrix δ' precipitates.

From observations of the decreasing number density of δ' precipitates on ageing, it was concluded that the increase in precipitate size with time was due to a coarsening mechanism, rather than a growth mechanism, and so plots of average precipitate radius against time$^{1/3}$ were made for all ageing temperatures. For the compound precipitates, the radius used was the radius of the whole particle minus the radius of the inner zirconium-rich precipitate as then a comparison could be made of the coarsening characteristics of both types of δ'. Fig. 3a shows the data for the coarsening of these two dispersions for a temperature of 433 K and it can be seen that within the limits of experimental scatter there is no distinguishable difference between the two. This was also the case for ageing temperatures of 443 and 453 K and thus Figs. 3a, b and c show only the mean coarsening rate for both types of δ' dispersion. It can be seen that Lifschitz–Wagner kinetics are being obeyed at these three temperatures and using the gradients of the lines shown, an activation energy for coarsening of $120 \pm 20\,kJ\,mol^{-1}$ is obtained.

For an ageing temperature of 473 K (Fig. 3d), the rate of increase in size with time of both types of δ' precipitate is still comparable between the two, thus again only the mean coarsening rate is shown. This is in contrast to the behaviour at 513 K (Fig. 3e), where a distinct difference in the coarsening characteristics of the two sorts of precipitate is seen at longer ageing times. As the size of the compound precipitate increases, it appears that its rate of coarsening decreases so that the precipitate seems to be tending towards a limiting size.

The rate of coarsening at these higher ageing temperatures is much greater than that seen at the lower ageing temperatures and this must be due, in part, to the effects of coalescence between the δ' in the matrix with other matrix δ' or the δ' of the compound precipitates. Fig. 4a shows these two types of particle coalescence in material that has been aged for 96 h at 513 K. The original spherical compound precipitate formed on Al_3Zr particle A has coalesced with two adjacent matrix δ' particles to form the oval compound precipitate seen. Evidence of coalescence between matrix δ' can also be seen, and an example of this is shown arrowed in this micrograph. Occasionally, coalescence of two compound precipitates could be observed although this was a rare event due to their low number density. However, Fig. 4b shows an area in material aged for 4 h at 553 K where coalescence between compound precipitates

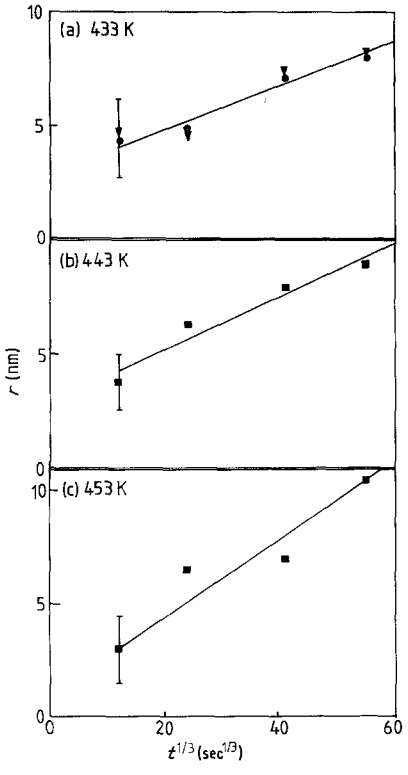

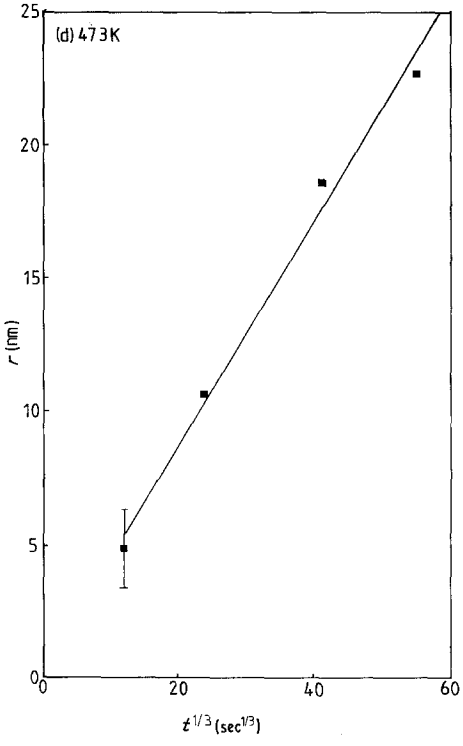

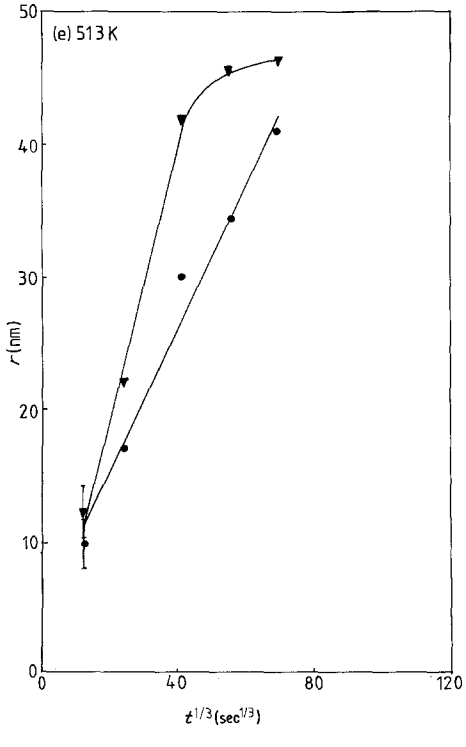

Figure 3 Coarsening plots of average precipitate radius, r, against (time)$^{1/3}$, $t^{1/3}$, for ageing temperatures between 433 and 513 K. ▼ interfacial δ', ● matrix δ', ■ mean of both dispersions of δ'.

would be viable. In thick areas of the foil it is difficult to ascertain, without the use of stereo techniques, whether the images of precipitates are merely overlapping through the thickness of the foil or genuinely coalescing. As coalescence became a more common event, the variation in precipitate size for a particular ageing treatment increased significantly, as would be expected.

Both matrix and interfacial δ' was visible after ageing for 30 min and 4 h at 553 K; however, for the longer ageing times used at this temperature, neither of these could be seen. There was an increased volume fraction of the δ phase in these specimens and thus it appeared that the metastable δ' had dissolved and the equilibrium δ phase had precipitated after 20 h at 553 K. The size of the compound precipitates seen in the specimen aged for 4 h at 553 K were comparable with those after an ageing time of 96 h at 513 K, i.e. in the region of the limiting size of precipitate seen. Loss of coherency of both the matrix δ' and the compound precipitates was also seen after ageing for 4 h at 553 K as shown in Fig. 4c where interfacial dislocations can be seen around the δ'/matrix interfaces and the δ'/Al_3Zr interface for Al_3Zr particles A and B. Particle C is a matrix

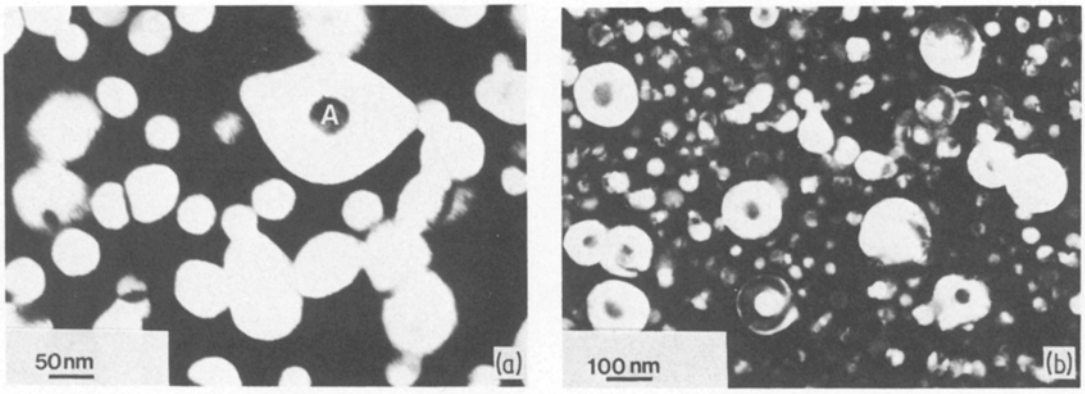

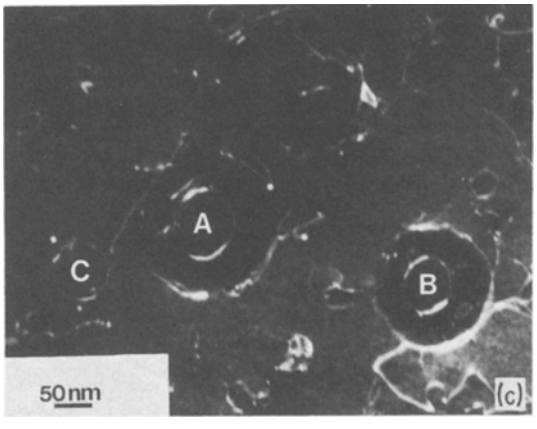

Figure 4 (a) Particle coalescence between matrix δ' and compound precipitate A and also between adjacent matrix δ' particles (arrowed); 513 K for 96 h. (b) coalescence between compound precipitates may be occurring in this region; 553 K for 4 h. (c) Weak beam micrograph showing interfacial dislocations for compound precipitates A and B and matrix δ' particle C; 553 K for 4 h.

δ' particle which also appears to have an interfacial dislocation surrounding it.

3.4. Boundary effects

3.4.1. Al_3Zr particles on boundaries

Some of the Al_3Zr precipitates situated on subgrain boundaries were seen to have an asymmetrical distribution of surrounding δ' precipitate as shown in Figs. 5a and b after ageing at 433 K for 48 h and 513 K for 4 h, respectively. The boundary is arrowed in each case and it may be seen that there is more interfacial precipitate on the side of the Al_3Zr particle furthest away from the boundary. In other cases, it appeared that there had been some boundary migration and the Al_3Zr particles were acting as pinning points, then the absence of precipitate on the boundary side of the Al_3Zr particle was even more pronounced.

3.4.2. Discontinuous reaction

The discontinuous reaction observed in binary alloys by Williams and Edington [7] was seen in this ternary alloy at temperatures between 433 and 473 K. Fig. 5c shows the reaction observed after an ageing treatment of 48 h at 433 K and the original position of the boundary is marked. As the boundary has migrated, it has taken the spherical δ' precipitates into solution and precipitated them as lamellae of δ' with the same orientation relationship to the matrix as before. In this case, it can be seen that the boundary has been pinned by the Al_3Zr particles denoted a and b. The δ' distribition ahead of the advancing boundary may also be seen using these particular diffracting conditions, and as expected both matrix and interfacial δ' can be imaged. A matrix δ' PFZ can also be observed ahead of the advancing boundary, as can a δ particle that has nucleated on the boundary.

An example of the same reaction is seen in Fig. 5d after 4 h at 473 K but this time the boundary appears to have broken away from the pinning Al_3Zr particle (marked X on the line of the original boundary). The usual lamellae of δ' can be seen and the asymmetrical interfacial δ' distribution around the Al_3Zr particle X is consistent with its original position pinning the boundary. Here it appears that the Al_3Zr particle has played no part in the discontinuous reaction.

4. Discussion

The results obtained in this study can be summarized as follows:

1. The Al_3Zr precipitation characteristics in a

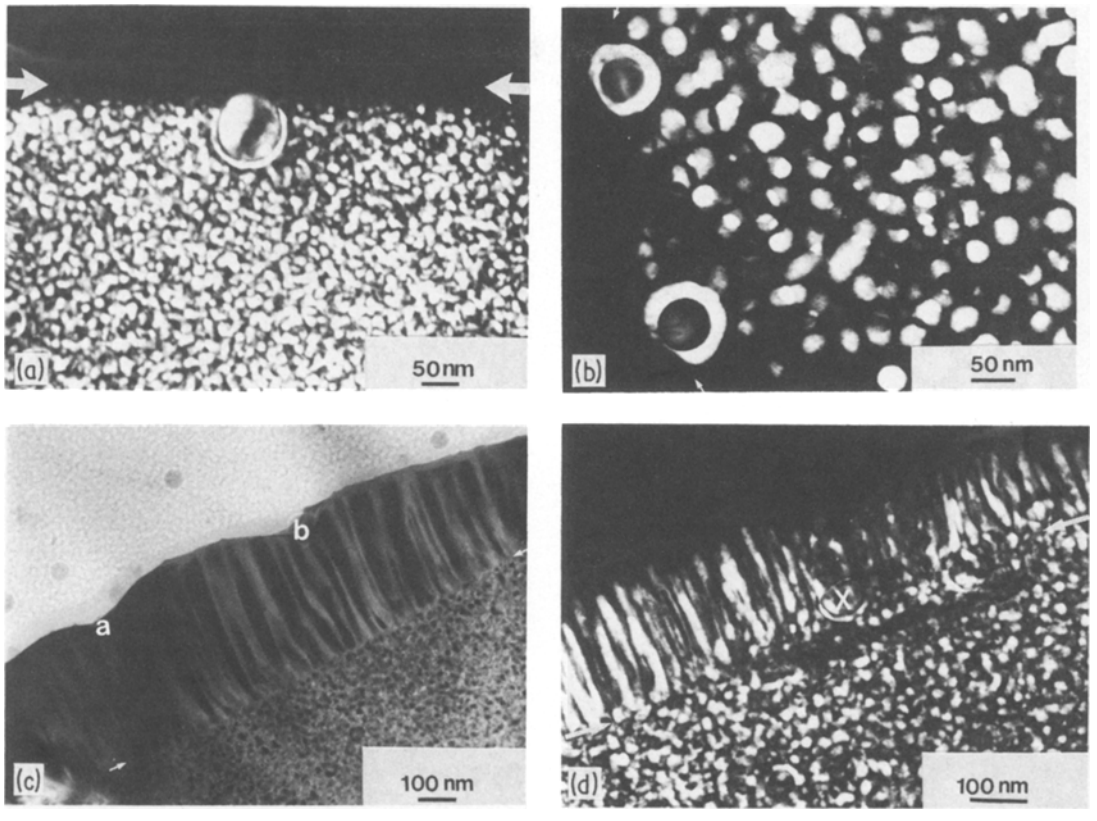

Figure 5 Asymmetrical distribution of δ' around Al_3Zr particles on subgrain boundaries (arrowed). (a) 433 K for 48 h; (b) 513 K for 4 h; (c) discontinuous reaction interface being pinned by Al_3Zr particles a and b. Original position of boundary is shown arrowed, 433 K for 48 h; (d) discontinuous reaction occurring after boundary has broken away from Al_3Zr particle X. Original position of boundary is shown arrowed 473 K for 4 h.

ternary Al–Li–Zr alloy resemble those reported in an Al–Zr binary of similar zirconium content.

2. The precipitation of δ' in the ternary system occurs both homogeneously in the matrix and on the Al_3Zr/matrix interface in the temperature range 433 to 553 K.

3. The coarsening of both distributions of δ' obey Lifshitz–Wagner kinetics for the lower temperatures in this range and an activation energy has been calculated that correlates with previously reported values for the binary alloy.

4. The distribution of interfacial δ' is symmetrical around Al_3Zr particles within a subgrain, yet depleted on the boundary side of pinning Al_3Zr particles.

The solution heat treatment used in this study was effectively a lithium solutionizing treatment, as the Al_3Zr dispersion was not significantly changed by it. The kinetics of Al_3Zr dissolution are very slow and in order to dissolve these precipitates, a much longer solution treatment would be needed. However, the resulting lithium loss, even from bulk specimens, would make such a treatment unsatisfactory for the purposes of this study.

The Al_3Zr precipitates seen were all of a spherical morphology, with none of the rod-shaped or plate-like precipitates that were observed by Nes in the binary 0.18% Zr alloy [6]. The precipitates appeared to be semicoherent which correlates with previous observations of Al_3Zr precipitates of a similar size [6, 10]. As expected, it seems that the addition of zirconium to the alloy has had a significant effect on the recrystallization behaviour as a binary Al–Li alloy has been found to be fully recrystallized after solution treating for shorter times at lower temperatures [7, 11].

The precipitation of matrix δ' appeared to show the same characteristics as the 3% Li binary alloys that have been studied previously [7, 12]. The number density and volume fraction seen

correlate well with those seen in the binary; thus it appears that there is little interaction between lithium and zirconium in solution. The chemical analysis data show that there is no evidence for the presence of zirconium in the interfacial δ' precipitate which suggests that zirconium is not incorporated into the precipitating δ'. The coarsening of the matrix δ' appears to follow the same trends as that seen previously in the binary alloy [7] with particle coalescence and heterogeneous coarsening (on dislocations and on boundaries as a discontinuous reaction) being seen after the ageing treatments described. It thus seems that the behaviour of the ternary alloy can be considered as an amalgamation of the behaviour of the two constituent binary alloys as a result of this negligible chemical interaction between lithium and zirconium in either the precipitate or solute state.

However, the nucleation of δ' on the semi-coherent Al_3Zr/matrix interface concomitant with nucleation of δ' in the matrix can be considered as a physical interaction between these two precipitates. Nucleation on pre-existing second phase particles has been seen in many materials (e.g. [13]), and it can be explained by considering the surface area of the precipitates formed. The associated reduction in interfacial energy resulting from precipitation at a pre-existing interface compared to homogeneous nucleation in the matrix can be calculated [13]. It must also be remembered that the matrix around the Al_3Zr particle may be enriched in lithium as a result of its formation. In this study, however, these effects would be negligble due to the homogenization resulting from the solution heat treatment at a temperature where the diffusion of lithium is fast.

As the interfacial δ' coalesces to form a complete shell, the compound precipitate will act as though it was wholly δ' and thus coarsen like a δ' particle of increased radius. The PFZ seen around the precipitates is a consequence of this, as the coarsening will occur at the expense of the surrounding smaller matrix δ'. The activation energy for the low-temperature coarsening of the compound precipitates is similar to that for the matrix δ', thus it appears that the two types of precipitate are coarsening by the same mechanism. The value obtained correlates with the previously reported activation energy for binary alloy δ' coarsening of $121 \pm 17\,kJ\,mol^{-1}$ [7] and $138 \pm 2\,kJ\,mol^{-1}$ [4], which are similar to the reported activation energies for volume diffusion of lithium in solution [4]. Thus it appears that both precipitate dispersions coarsen by a mechanism involving the diffusion of lithium through the matrix.

The observation of a limiting size for the compound precipitates could be an artefact of the foil thickness; however, it is at this limiting size that the first signs of loss of coherency of the δ'/matrix interface are seen. Further ageing seems to result in δ' dissolution and the precipitation of the equilibrium stable δ phase. This is in agreement with the coherent δ' phase boundary defined by Williams and Edington for binary Al–Li alloys [7] as at these concentrations of lithium the coherent δ' solvus was almost coincident with the ordinary δ' solvus. Loss of coherency of the matrix δ' and the interfacial δ' appears to occur by pick-up of matrix dislocations and further work is in progress to ascertain the size range over which coherency is lost more clearly.

The asymmetrical interfacial δ' distribution around Al_3Zr particles on boundaries can be explained by considering the line tension of the boundary. Any increase in size of the pinning precipitate necessitating an increase in length of boundary would be energetically unfavourable, thus nucleation and coarsening of interfacial δ' is suppressed on the boundary side of the precipitate.

The observation of the discontinuous reaction at temperatures between 433 K and 473 K but not at higher temperature is in contrast to behaviour in the Al–Li binary where the reaction was seen at temperatures up to 523 K [9]. The presence of Al_3Zr particles that can pin the boundaries will cause the mobility of the boundaries to be reduced which will aid in suppressing the reaction; however, it has been observed that the boundary can break away from these particles and act as a discontinuous reaction interface. The absence of any chemical interaction between Al_3Zr particles and the δ' discontinuous reaction is to be expected in the light of the previous observations of this study concerning the lack of chemical interaction between lithium and zirconium in this ternary alloy. The matrix δ' PFZ seen ahead of the discontinuous reaction interface is interesting as it is generally considered that a discontinuous reaction occurs in the moving interface only and needs no diffusion of solute

from ahead of the interface. However, a similar effect has been seen in a stainless steel [14] and this was explained by the precipitation of equilibrium phases behind the reaction interface causing a net depletion of solutes. In the present alloy, it is most likely that the precipitation of the δ particle further along the discontinuous interface has caused a depletion of lithium such that a PFZ results, but there is a possibility that the discontinuous reaction may only be able to occur after suitable lithium diffusion from the matrix ahead. Further work is necessary to clarify the exact reason for the PFZ observed both on the ternary and by comparison with observations in binary Al–Li alloys.

Acknowledgements

The authors are grateful to Professor R. W. K. Honeycombe FRS for the provision of laboratory facilities. Financial support from the Science and Engineering Research Council and the Banbury Laboratories of Alcan International is gratefully acknowledged. Material was supplied by Alcan International and much valuable advice from Dr D. M. Ball and Dr D. Field of Alcan is also acknowledged. Finally, it is a pleasure to thank Dr A. J. Porter and Dr R. A. Ricks for valuable discussions.

References

1. T. H. SANDERS, JR and E. A. STARKE, JR (EDS), "Aluminium–Lithium Alloys" (Metallurgical Society AIME, New York, 1981).
2. E. A. STARKE, Jr, T. H. SANDERS, Jr and I. G. PALMER, *J. Metals.* **33** (1981) 24.
3. K. K. SANKARAN and N. J. GRANT, in "Aluminium–Lithium Alloys", edited by T. H. Sanders, Jr and E. A. Starke, Jr (Metallurgical Society AIME, New York, 1981) p. 205.
4. B. NOBLE and G. E. THOMPSON, *Met. Sci. J.* 5 (1971) 114.
5. A. GYSLER, R. CROOKS and E. A. STRIKE, Jr, in Proceedings of the 75th International Light Metals Congress, Leoben-Vienna, Austria (1981) p. 50.
6. E. NES, *Acta Metall.* **20** (1972) 499.
7. D. B. WILLIAMS and J. W. EDINGTON, *Met. Sci.* 9 (1975) 529.
8. D. B. WILLIAMS, in "Aluminium–Lithium Alloys", edited by T. H. Sanders Jr and E. A. Starke, Jr (Metallurgical Society AIME, New York, 1981) p. 89.
9. D. B. WILLIAMS and J. W. EDINGTON, *Acta Metall.* **24** (1976) 323.
10. A. J. PORTER, P. L. MAKIN and B. RALPH, in Proceedings of the 41st EMSA Conference, Phoenix, August 1983, edited by G. W. Bailey (San Francisco Press, California, 1984) p. 242.
11. P. L. MAKIN, CPGS dissertation, University of Cambridge (1983).
12. D. B. WILLIAMS, PhD thesis, University of Cambridge (1974).
13. R. A. RICKS, G. S. BARRITTE and P. R. HOWELL, in Proceedings of the Conference on Solid-Solid Phase Transformations, Pittsburgh, Pennsylvania, USA, 10–14 August 1981, edited by H. Aaronson *et al.* (AIME, New York, 1982) p. 463.
14. R. A. RICKS, *Met. Sci.* (in press).

Received 4 November
and accepted 24 November 1983